JOURNAL OF MOLECULAR SPECTROSCOPY 158, 27–39 (1993)

The Ground State of the $CuCl_2$ Molecule from Laser-Induced Fluorescence

A. J. ROSS, R. BACIS, A. J. BOUVIER, S. CHURASSY, J.-C. COSTE, P. CROZET, AND I. RUSSIER

Laboratoire de Spectrométrie Ionique et Moléculaire, Bâtiment 205, Université Lyon I, 43, Boulevard du 11 novembre 1918, 69622 Villeurbanne Cedex, France

The ground state of $CuCl_2$ has been studied by laser-induced fluorescence spectroscopy. $CuCl_2$ vapor, produced in a sealed quartz cell, was excited with a ring laser operating with DCM or Rhodamine 6G dye. Fluorescence in the region 11 000–15 500 cm^{-1} was recorded on a Fourier transform spectrometer. Transitions to about 40 vibrational levels of the ground state have been observed. These are identified as vibrational progressions in the symmetric stretch ($0 \leq v_1'' \leq 12$) in combination with even quanta of the antisymmetric stretch ($v_3'' = 0, 2, 4, 6$ or 8) occurring to the $^2\Pi_g$ ground state. © 1993 Academic Press, Inc.

INTRODUCTION

In an earlier paper (*1*), we presented the results of a laser-induced fluorescence experiment, in which the red lines of a krypton ion laser were used to excite $CuCl_2$ vapor. The spectra were composed of resolved doublets and gave a vibrational interval varying from 356 to 368 cm^{-1}, in close agreement with the ab initio predictions made by Bauschlicher and Roos (*2*), but no attempt was made to analyse these spectra any further. The quantity of information to be obtained from them was very limited, and we have since pursued the problem with a tunable laser source. We aimed to probe systematically a set of vibrational and rotational levels in $CuCl_2$ with the laser, and to record fluorescence from these levels to the low-lying ligand field states. We relied on the selectivity of the laser line to achieve a rotationally simple spectrum from a hot source: the absorption spectrum of $CuCl_2$ recorded under these conditions is sufficiently congested as to appear to be a continuum (*3*). We hoped that such an experiment would allow us to observe all the vibrational modes of the ground state of $CuCl_2$, predicted to be $^2\Pi_g$ (*2*), and also to locate the higher lying ligand field states, $^2\Sigma_g^+$ and $^2\Delta_g$. Our choice of excitation wavelengths has been such that we have excited rotational energy levels of only two vibrational levels of the upper state, assumed to be the charge transfer state $^2\Pi_u$, and, to date, we have analyzed fluorescence to only one low-lying electronic state, which we believe to be $^2\Pi_{g(3/2)}$. We have observed only two of the normal vibrational modes, namely, ν_1'' and ν_3'', which are respectively the symmetric and antisymmetric stretching vibrations of a symmetric triatomic molecule.

The absence of the degenerate bending vibration in our spectra contrasts with results obtained from electronic spectra of nickel dichloride, which is the closest comparison in terms of electronic structure that we could find in the literature. A low-resolution dispersed fluorescence experiment in $NiCl_2$, performed by Zink *et al.* (*4*), showed long progressions in v_1'' and combinations of nv_1'' with $2v_2''$ following excitation by the

0022-2852/93 $5.00

364-nm line from an argon ion laser. Other combinations were also assigned in this work, including combinations of nv_1'' with $2v_3''$, but these bands were relatively weak, and no higher levels involving the antisymmetric stretch, v_3'', were assigned. An extensive investigation of the excitation spectra of nickel dichloride around 360 nm (*5*) and 460 nm (*6*) obtained with a cold molecular beam also failed to give much information about the antisymmetric stretching vibration. The vibrational structure in the spectrum of $NiCl_2$ was particularly clear in Ref. (*6*); the obvious features were a long progression in v_1', and a short progression involving the excitation of 2 quanta of the bending vibration, v_2. Some spin–orbit structure was apparent in these spectra, and some very weak bands were tentatively assigned as sequence bands in the antisymmetric stretching vibration, with $v_3' = v_3'' = 1$. In copper dichloride, we observed strong transitions to combination levels of $nv_1'' + (\text{even})v_3''$, but no such combinations with $(\text{even})v_2''$, or sequences involving the bending vibration were noted.

In any case, it seems that an investigation of dispersed fluorescence from a "hot" source is likely to prove useful in the study of transition metal dihalides (for which few high-resolution spectra exist), as the information obtained covers high-lying rotational and vibrational energy levels of the ground state, and so complements such data as could be obtained from a cold molecular beam experiment. A full analysis of the rovibrational structure of the transition metal dihalides would provide an important clue to their electronic and geometric structure in the gas phase, adding to information from elaborate ab initio calculations, or measurements of the deflection of molecular beams in a inhomogeneous electric field (*7*), which have been used to determine whether or not an MX_2 molecule is linear. In this instance, an understanding of the electronic spectra of copper dichloride should also clarify the problem, presented in Refs. (*1, 8*), concerning the origin of the red and infrared emission observed when hot copper, chlorine, and metastable oxygen react together. This emission was first reported by Yoshida *et al.* in 1989 (*9*), and has been extensively studied since then (*10–13*). There seems to be agreement that $CuCl_2$ is at least partly, if not wholly, responsible, but an improvement in the spectroscopic data for copper dichloride would add weight to this hypothesis.

In this paper, we describe the experimental conditions used to record electronic spectra of copper dichloride vapor at high resolution, and then give results of the numerical treatment of the spectral lines which have been assigned to the $^{63}Cu^{35}Cl_2$ isotopomer. A simple model which takes into consideration the symmetric and antisymmetric stretching vibrations and their anharmonicities, but allows for no other interaction, is used to derive the vibrational and rotational constants of this molecule.

EXPERIMENTAL DETAILS

We prepared $CuCl_2$ by sealing about 10 mg of copper powder (99.9% pure) with enough chlorine gas to react stoichiometrically to produce $CuCl_2$ in a quartz cell equipped with Brewster windows and a sidearm. The cell was placed in an oven which allowed the main body of the cell to be maintained at 750°C (at which temperature copper dichloride dimer (*14*) is reported to be fully dissociated), while the sidearm temperature was lower, so that the vapor pressure in the cell could be controlled. Although we were concerned that other stable species such as CuCl and Cu_3Cl_3 might also be formed in the source, and tried to add excess chlorine to prevent this, we found in practice that the quality of the spectra was not greatly affected by differences in the original mixture; good spectra were obtained with either copper or chlorine in slight excess.

Fluorescence spectra were excited with a Spectra Physics ring dye laser (380 D) operating single mode with DCM or Rhodamine 6G dye, and recorded on a Bomem DA3 Fourier transform spectrometer using a silicon avalanche detector. The dye laser wavelength was continuously monitored with a Fizeau wavemeter (Laser Technics 100). The setup is shown schematically in Fig. 1.

The spectra were recorded twice, once at very low resolution, and then at higher resolution. The low-resolution survey spectra were important because they enabled us to decide which laser wavelengths actually resulted in a discrete spectrum. Given the expected complexity of the electronic spectrum of $CuCl_2$, and the presence of both possible isotopic species of chlorine and copper in our source, we were not particularly surprised to find that the total fluorescence signal from the cell was totally insensitive to the choice of wavelength, even with a laser linewidth of about 50 MHz. The survey spectra showed us that while any laser line could excite a broad continuum emission, only a few select frequencies produced the same continuum with a discrete structure superposed on it. Having found a potentially interesting laser wavelength, we went on to record the fluorescence spectrum from 11 000–15 400 cm^{-1} at an apodized resolution of 0.07 cm^{-1}, using an appropriate optical filter to attenuate or eliminate the laser line. The recording time was typically 2 hr.

EXPERIMENTAL RESULTS

The first obvious result was the sensitivity of the discrete part of the spectrum to the choice of the exciting laser wavelength, as illustrated in Fig. 2. Our first high-resolution recordings of the discrete part of the spectrum, which were obtained using the DCM dye, showed a very simple rotational structure (P, R doublets with no relaxation), and an apparently straightforward vibrational pattern (see Fig. 3a). It was difficult to ascertain which isotopomer we were seeing, and also to establish rotational numbering from so few lines. In order to facilitate the subsequent analysis, we deliberately chose to use small intervals between our excitation lines, hoping to excite neighboring rotational levels of a single upper state vibrational level in successive

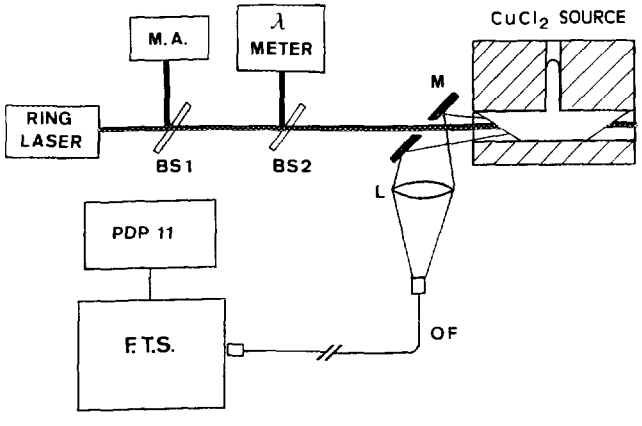

FIG. 1. Experimental setup. BS1 and BS2 are beamsplitters, used to direct part of the laser beam to a mode analyser (MA) and to a Fizeau wavemeter. M is a pierced mirror which collects backward fluorescence from the $CuCl_2$ cell. L is a quartz lens, $f = 20$ cm. OF represents 10-m fused silica optical fiber, which transfers the fluorescence to the Fourier transform spectrometer. The cell is maintained at 750°C, with the sidearm at 550°C.

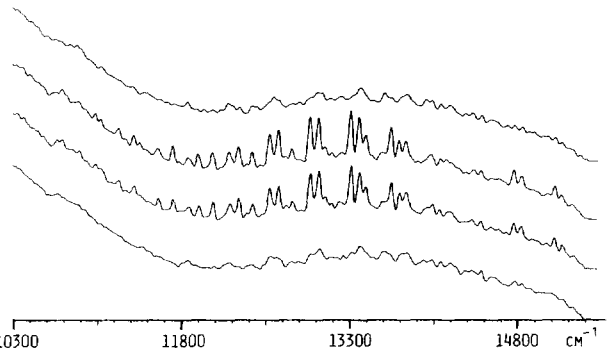

FIG. 2. A series of low-resolution ($\sim$30 cm^{-1}) spectra, showing the sudden appearance of a discrete spectrum as the excitation wavenumber changes. From top to bottom, the laser was set at 16 229.26, 16 229.23, 16 229.20, and 16 229.16 cm^{-1}.

recordings. We concentrated on regions with the laser close to 657 and 647 nm (DCM, with average output power $\sim$350 mW), and then worked at higher excitation energies around 607 nm (Rhodamine 6G, power $\sim$200 mW). The discrete fluorescence was spread over about forty vibrational levels of the ground state. The obvious vibrational structure seen in the fluorescence spectra excited by DCM was a progression in the symmetric stretch vibration (Fig. 3a), but a more complex vibrational pattern was apparent in the R6G spectra (Fig. 3b).

We found that most of our data could be understood in terms of fluorescence from a $T'_{v,J}$ level to the ground state as progressions in the symmetric stretching vibration, occurring in combinations with even quanta of v''_3 (the antisymmetric stretch vibration). The lower energy laser lines (DCM) excited a vibrational level about 15 880 cm^{-1} above the lowest level observed in fluorescence, and produced emission essentially to $v''_3 = 0$ and 2, as illustrated in Fig. 3a. The Rhodamine 6G excitations were to a different upper state vibronic level, about 370 cm^{-1} higher than the other, and resulted in emission to higher combinations of v''_3: we have observed bands with $v''_3 = 0$, 2, 4, 6, and 8 (Fig. 3b). We assign this emission to part of the $^2\Pi_u$–$^2\Pi_g$ transition in $CuCl_2$: the only electronic state likely to be excited by the laser, according to the ab initio calculations of Ref. (*2*), is $^2\Pi_u$, and the *P*, *R* doublets observed in fluorescence are consistent with a $^2\Pi$–$^2\Pi$ transition. The question remains as to which spin–orbit component is observed. The apparent lack of lambda doubling in the regular parts of the spectrum, even at high *J* values, tends to suggest that we have observed the $^2\Pi_{u(3/2)}$–$^2\Pi_{g(3/2)}$ transition rather than the $^2\Pi_{u(1/2)}$–$^2\Pi_{g(1/2)}$ transition (lambda doubling is usually larger in the $\frac{1}{2}$ than in the $\frac{3}{2}$ component of a $^2\Pi$ state). However, this can only be a hypothesis until the other component of the $^2\Pi_g$ state is observed and characterized, and for the time being we have considered rotational lines to have an effective rotational quantum number *J*, and have neglected the effects of the orbital angular momentum quantum number Ω. Through lack of information on ν_2, we have also been obliged to neglect the contribution to angular momentum l_2, which comes from the degenergate bending vibration. Given the absence of progressions in even quanta of the bending vibration in our spectra, we consider it likely that both the upper and lower electronic states of $CuCl_2$ are linear in geometry.

From our measurements of the antisymmetric stretch ν''_3, we were able to recognize the different isotopomers of $CuCl_2$ present in our source. This was important, because

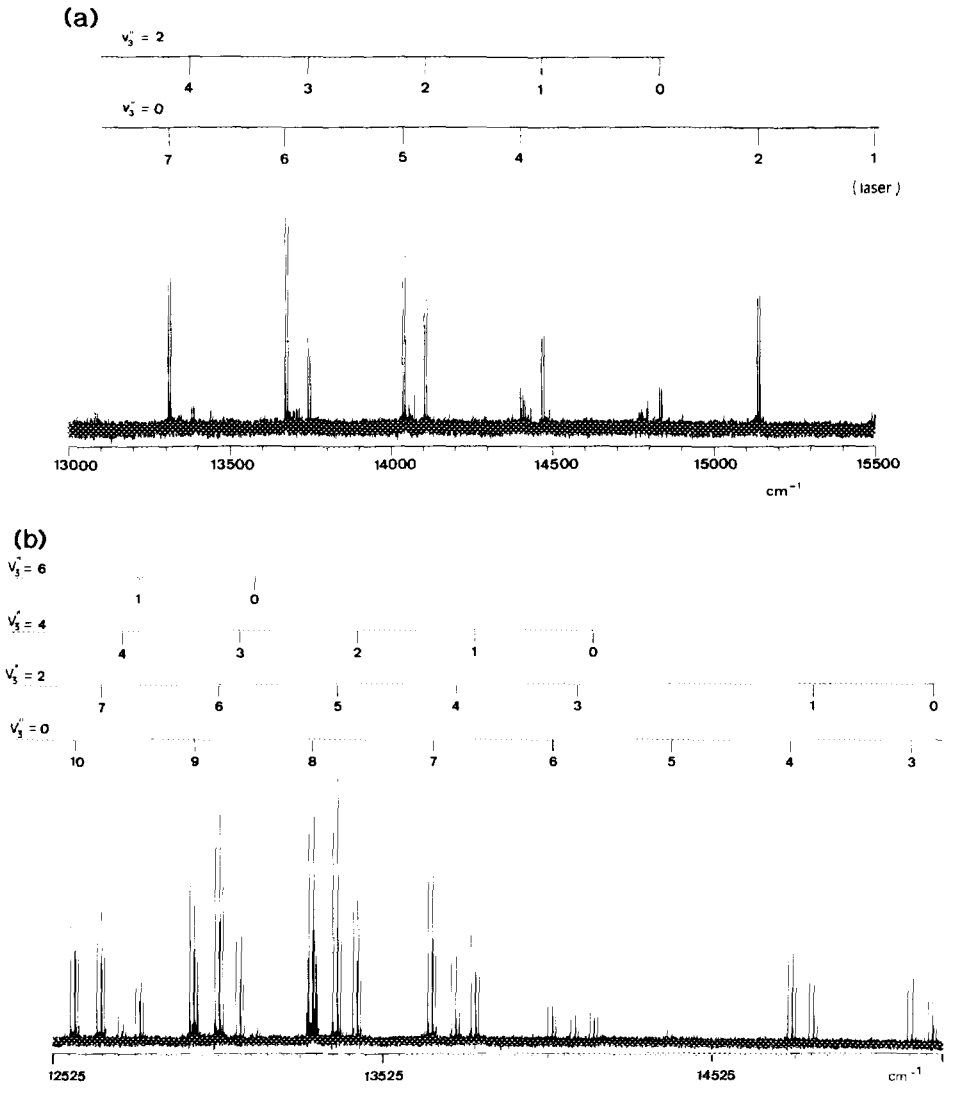

FIG. 3. Examples of resolved fluorescence spectra, giving vibrational numbering in v_1'' at given v_3''. (a) Spectrum recorded at 0.08-cm^{-1} resolution with the ring laser operating at 15 502.3 cm^{-1} with DCM dye, exciting $J' = 31\frac{1}{2}$ in "Level 1" (see text). (b) Spectrum recorded at 0.07-cm^{-1} resolution with the ring laser operating at 16 236.60 cm^{-1} with R6G dye, exciting $J' = 46\frac{1}{2}$ and $63\frac{1}{2}$ in "Level 2" (see text).

in some of the DCM spectra, in which only the symmetric stretch progressions were noted, we were unable to distinguish between the two isotopes of copper. So far, we have observed $^{63}Cu^{35}Cl_2$, $^{65}Cu^{35}Cl_2$, $^{63}Cu^{35}Cl^{37}Cl$, and $^{65}Cu^{35}Cl^{37}Cl$, but at present most of our data relates to the most common species, $^{63}Cu^{35}Cl_2$. The analysis presented here therefore treats only this isotopomer, but work is in progress to acquire a comparable data set for the other species of $CuCl_2$.

Data Reduction

In some respects, we suffered from the oversimplification of the rotational structure in our spectra. It was very easy to recognize the spectral features which appeared, but

TABLE I

Range of J'' Values Observed in the Ground State Vibrational Levels

v_1'' \ v_3''	0	2	4	6	8
0	16½ - 75½	8½ - 110½	8½ - 110½	35½ - 75½	
1	25½ - 75½	8½ - 110½	6½ - 110½	8½ - 75½	41½ - 73½
2	18½ - 57½	16½ - 110½	7½ - 110½	8½ - 75½	41½ - 75½
3	7½ - 110½	16½ - 110½	8½ - 110½	6½ - 75½	47½ - 73½
4	7½ - 110½	7½ - 110½	9½ - 110½	8½ - 75½	45½ - 64½
5	18½ - 110½	7½ - 75½	35½ - 110½	8½ - 75½	45½ - 62½
6	8½ - 75½	7½ - 75½		43½ - 75½	
7	7½ - 75½	7½ - 75½			
8	7½ - 75½	8½ - 75½			
9	7½ - 110½	7½ - 75½			
10	7½ - 110½	8½ - 75½			
11	9½ - 110½	8½ - 75½			
12	8½ - 75½	45½ - 64½			

it was much more difficult, if not impossible, to assign all the quantum numbers with certainty, particularly because the regularity of the spectra seen at a first glance (Figs. 3a and 3b) is in reality less than perfect—small perturbations abound in the higher v'' levels. By accumulating some 50 spectra, we eventually assembled the pieces of the puzzle which could be made to fit together, and produced a model which could account for most of the lines observed. However, it must be said that our analysis is not exhaustive. Not having observed the first lines of the rotational bands, we cannot categorically state which spin–orbit component we have studied, neither can we justify fully the vibrational numbering scheme given. One obvious remedy would be to use isotope effects to confirm the numbering presented here, and we intend to work with enriched $^{37}Cl_2$ to study $Cu^{37}Cl_2$ in the near future. For the moment, we have assigned a few lines to $^{65}Cu^{35}Cl_2$, which tends to confirm the numbering for the antisymmetric stretch, but is unfortunately of no help for the numbering of the symmetric stretch levels. But we have accrued a data set of some 2000 lines assigned to $^{63}Cu^{35}Cl_2$, and can derive from this a fair description of the lower electronic state observed. The rotational analysis was based on the first six levels of the symmetric stretching vibration, which had regular rotational and vibrational spacings. The rotational quantum number defined in this way allows us to represent the rotational energy levels by a simple $B_{\text{eff}}J(J+1) - D_{\text{eff}}J^2(J+1)^2$ expression, and ignores the correction for the (unknown) Ω and the bending vibration's contribution to the total angular momentum.

The extent and number of perturbed lines in the higher vibrational levels observed led us to exploit the data available in two different ways. The first was a fit on a band-by-band basis to a set of effective spectroscopic constants, and the second was to fit the data to a very small set of parameters, which expressed the rovibrational energy

levels by a polynomial expression describing the rotation, symmetric, and antisymmetric stretching vibrational energies simultaneously. In both cases, the upper state was reduced to a simple expression in T', B', and D' for the two observed vibrational levels, but no true analysis of the upper state has been attempted. The spread of rotational lines over the observed vibrational levels is indicated in Table I, but it is important to remember that a laser-induced fluorescence experiment does not afford a statistical distribution over rotational levels. In fact, we did not observe any lines at all with $76.5 < J' < 108.5$, but levels with $J' < 76.5$ were well represented.

The lines included in our data set came from two vibrational levels of what we have assumed to be the $^2\Pi_u$ state. The lower of the two, called level 1, gave a systematic Franck–Condon intensity minimum at $v_1'' = 3$ in our symmetric stretch fluorescence progression, and the higher (level 2) gave two such minima at $v_1'' = 3$ and 7. A small number of lines at high J were also observed as progressions in the symmetric stretch from another level, located about 330 cm^{-1} below level 1, always with $v_3'' = 0$. As we were unable to tell which copper isotope was observed, or confirm that exactly the same lower state levels were involved in these DCM-induced transitions, none of these lines were included in our data set. Using fluorescence to four regular lower state levels, we determined effective constants for these two upper state levels with respect to $G_{(v_1''=0,v_3''=0)}$, the lowest observed vibrational level of the ground state. We found:

level 1: $T' = 15882.155\ (5)$, $B' = 0.051764\ (9)$,
and $D' = 8.41\ (77) \times 10^{-9}\ cm^{-1}$;

level 2: $T' = 16257.092\ (3)$, $B' = 0.051330\ (9)$,
and $D' = 8.45\ (79) \times 10^{-9}\ cm^{-1}$.

From the intensity distribution in the progression in v_1'' with $v_3'' = 0$, we were tempted to consider these levels as $v_1' = 1$ and 2 in the upper state. However, the predicted vibrational spacing in the upper state is only 275 cm^{-1} (*2*), and the observed spacing, ~ 375 cm^{-1}, is closer to the upper state antisymmetric stretch frequency. So far, attempts to reproduce observed intensities with simple Franck–Condon overlap calculations have failed.

Band-by-Band Fit

This approach allowed lower state effective spectroscopic constants to be determined, and gives a fit to the observed lines to better than 0.01 cm^{-1} in the unperturbed levels. We proceeded by fixing the constants for the upper state levels to the values cited above, and in so doing fixed the energy origin to be the lowest observed vibrational level of the ground state. The numerical results are given in Table II. It becomes obvious that the evolution of the vibrational energies becomes irregular at $v_1'' > 7$ with $v_3'' = 0$, but levels of comparable energy with $v_3'' = 2$ are still reasonably regular. The set of levels with $v_3'' = 2$ becomes noticeably perturbed beyond $v_1'' = 6$, and the observed levels with $v_3'' = 4$, 6, and 8 appear reasonably regular throughout. It is also clear from this table that the values of the effective rotational constants are not greatly affected by these perturbations; their values vary in the usual way.

Some explanation is required concerning the levels for which the standard deviation of the fit is particularly large. These were characterized by the large number of extra lines observed in a few $v' \rightarrow v_1''$, v_3'' bands, illustrated, for instance, in Fig. 4. Trying to fit the lines in these bands to our simple model resulted in a distribution of residuals

TABLE II

Constants from Band-by-Band Fit of Fluorescence Lines of $^{63}Cu^{35}Cl_2$

v_1''	v_3''	G_{v_1,v_3} cm^{-1}	B_{v_1,v_3} cm^{-1}	$10^9 D_{v_1,v_3}$ cm^{-1}	N° lines	Rms. dev. cm^{-1}
0	0	0.0	0.058161 (3)	10.0	4	0.009
1	0	369.392 (3)	0.058024 (3)	7.8 (4)	9	0.003
2	0	737.755 (3)	0.057914 (7)	10.5 (17)	18	0.005
3	0	1105.140 (3)	0.057769 (1)	6.2 (1)	50	0.010
4	0	1471.471 (3)	0.057648 (1)	6.5 (1)	84	0.011
5	0	1836.788 (2)	0.057516 (1)	5.5 (1)	39	0.006
6	0	2201.083 (6)	0.057379 (6)	6.1 (10)	105	0.023
7	0	2564.354 (23)	0.057215 (7)	10.0	127	0.132
8	0	2926.450 (160)	0.057270 (56)	10.0	116	0.961
9	0	3288.026 (86)	0.057218 (22)	10.0	120	0.554
10	0	3647.980 (12)	0.057055 (6)	9.5 (6)	89	0.051
11	0	4007.137 (7)	0.056897 (3)	7.3 (3)	47	0.018
12	0	4365.262 (5)	0.056753 (4)	4.3 (7)	37	0.012
0	2	1042.005 (4)	0.057739 (2)	6.0 (2)	45	0.013
1	2	1406.267 (3)	0.057620 (1)	6.1 (1)	62	0.011
2	2	1769.493 (4)	0.057502 (3)	6.5 (2)	29	0.011
3	2	2131.680 (3)	0.057379 (2)	7.5 (1)	61	0.011
4	2	2492.690 (39)	0.057427 (20)	18.1 (18)	60	0.158
5	2	2853.004 (3)	0.057133 (2)	3.7 (4)	82	0.010
6	2	3212.052 (6)	0.057004 (4)	6.3 (8)	102	0.021
7	2	3570.065 (31)	0.056860 (27)	7.4 (46)	72	0.106
8	2	3926.810 (300)	0.056771 (86)	10.0	89	1.33
9	2	4283.164 (342)	0.056726 (105)	10.0	78	1.44
10	2	4637.790 (34)	0.056697 (27)	6.5 (46)	57	0.097
11	2	4991.582 (16)	0.056543 (12)	7.6 (20)	36	0.036
12	2	5344.303 (3)	0.056417 (1)	10.0	3	0.001
0	4	2074.366 (2)	0.057343 (1)	5.9 (1)	48	0.008
1	4	2433.585 (2)	0.057224 (1)	6.1 (1)	59	0.007
2	4	2791.753 (2)	0.057101 (1)	6.2 (1)	67	0.009
3	4	3148.835 (2)	0.056974 (9)	7.7 (1)	61	0.007
4	4	3504.892 (19)	0.057066 (62)	22.2 (49)	46	0.348
5	4	3859.885 (22)	0.056773 (9)	6.1 (6)	13	0.020
0	6	3097.104 (10)	0.056973 (6)	9.2 (9)	18	0.007
1	6	3451.393 (4)	0.056827 (3)	5.8 (5)	40	0.007
2	6	3804.548 (3)	0.056703 (2)	6.1 (4)	61	0.008
3	6	4156.506 (6)	0.056612 (6)	13.8 (10)	63	0.021
4	6	4507.220 (110)	0.056695 (36)	10.0	74	0.506
5	6	4857.481 (27)	0.056429 (7)	10.0	48	0.081
6	6	5206.296 (18)	0.056243 (10)	5.2 (13)	23	0.008
1	8	4459.689 (16)	0.056456 (1)	8.9 (1)	13	0.006
2	8	4807.880 (20)	0.056323 (11)	8.0 (1)	22	0.009
3	8	5154.764 (52)	0.056166 (12)	10.0	13	0.032
4	8	5501.228 (1)	0.056123 (1)	10.0	4	0.005

Note. The figures given in parentheses represent one standard deviation, in units of the last quoted digit. It was not always possible to determine the distortion constant, D_{v_1,v_3}. When necessary, we fixed D_{v_1,v_3} at 10^{-8} cm^{-1}, in which case no error is given.

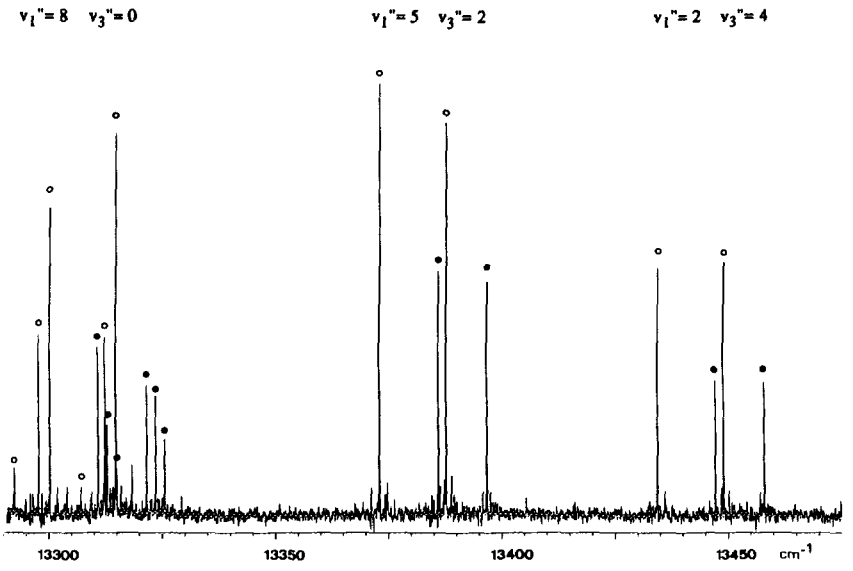

FIG. 4. Detail taken from Fig. 3b, showing obvious perturbations in the band with $v_1'' = 8$, $v_3'' = 0$, while the nearby $v_1'' = 5$, $v_3'' = 2$, and $v_1'' = 2$, $v_3'' = 4$ remain regular. The laser pumps both $J' = 46\frac{1}{2}$ and $63\frac{1}{2}$ in the upper state vibrational level. Fluorescence doublets from $J' = 46\frac{1}{2}$ are indicated by filled circles, and from $J' = 63\frac{1}{2}$ by open circles.

which was not random, but increased slowly with J. The calculated wavenumber was usually quite close to the average wavenumber of the lines of a given lower state rotational quantum number, as though we were seeing an exaggerated form of lambda-type doubling. This splitting of rotational levels, which is important in only 6 out of the 40 lower state vibrational levels we have observed, namely, (v_1'', v_3'') being (8, 0), (9, 0), (8, 2), (9, 2), (4, 4), and (4, 6), probably arises from strong interactions between the vibrational levels of the other ligand field states. The "other" spin–orbit component of the $^2\Pi_g$ state is expected to have very similar spectroscopic constants to the one we see, and to lie close in energy to it, and should thus influence even the lowest vibrational levels. According to the ab initio calculations in Ref. (*2*), the observed perturbed levels lie well below the $^2\Delta_g$ state, (situated approximately 5000 cm^{-1} above the ground electronic state), so the $^2\Sigma_g^+$ state remains the most likely candidate to undergo strong interactions with the $^2\Pi_g$ state in this way. Even so, interactions between a $^2\Pi_g$ and a $^2\Sigma_g^+$ state cannot account for all the observed extra lines, as up to eight lines are observed instead of the usual rotational doublet.

Polynomial Fit

In order to derive the vibrational constants for $CuCl_2$, we used a more compact set of parameters to represent the spectroscopic term values, by fitting the measured wavenumbers to an expression of the form $\nu_{\text{measured}} = T'_{(v',J')} - T''_{(v_1'',v_3'',J'')}$, in which the energy levels for the lower state were represented by

$$T''_{(v_1'',v_3'',J'')} = \omega_1(v_1 + 1/2) + x_{11}(v_1 + 1/2)^2 + x_{111}(v_1 + 1/2)^3 + \omega_3(v_3 + 1/2)$$
$$+ x_{33}(v_3 + 1/2)^2 + x_{333}(v_3 + 1/2)^3 + x_{13}(v_1 + 1/2)(v_3 + 1/2)$$
$$+ \{B_e - \alpha_1(v_1 + 1/2) - \alpha_3(v_3 + 1/2)\}J(J + 1) - DJ^2(J + 1)^2.$$

However, the results from the band-by-band fit had made it obvious that an attempt to represent the full data set by such a simple expression would be doomed to failure, as the distribution of errors in the recalculated wavenumbers is not at all random. Obviously, the interaction which allows us to see multiple lines in certain bands (Fig. 4) causes major problems in an overall representation of the energy levels observed. We thus restricted the data set for this polynomial approach to a smaller number of bands, with a view to obtaining parameters which have physical significance for the normally behaved levels. The results obtained are given in Table III. Two series of constants are given. The first is the fit of a rather restricted set of data, concerning essentially the lower state levels with $v_1'' < 8$, but from which fluorescence to the levels ($v_1'' = 4$, $v_3'' = 6$), ($v_1'' = 4$, $v_3'' = 4$), and ($v_1'' = 7$, $v_3'' = 2$) had also been eliminated. This data set contains essentially unperturbed lines, and the rms error reflects this (0.14 cm^{-1} for 1517 input lines). The bands which were removed from the total data set were the ones which had either a rms error in the band-by-band fit greater than 0.15 cm^{-1}, which was symptomatic of levels in which the rotational lines appeared as doublets (or higher multiplets), particularly at high J, or those for which the vibrational term energy seemed irregular. For example, the lower state level with ($v_1'' = 7$, $v_3'' = 2$) has a modest rms error in the band-by-band fit, but when included in the data set for a fit to a polynomial expression, almost all the fluorescence lines to this level were recalculated about 0.4 cm^{-1} from their measured wavenumbers. This reflects a shift of the vibrational energy as a whole. The larger data set appearing in Table III contains levels with $v_1'' = 10$, 11 and 12 in addition to the data contained in the small

TABLE III

Molecular Constants (in cm^{-1}) of $^{63}Cu^{35}Cl_2$ Obtained from Fits to Polynomial Expressions

	Small data set ($v_1'' < 8$)	Larger data set ($v_1'' < 12$)
ω_1	371.669 (11)	371.885 (22)
x_{11}	- 0.5143 (10)	- 0.5604 (38)
x_{111}		2.7 (2) x 10^{-3}
ω_3	525.681 (9)	525.878 (25)
x_{33}	- 1.1762 (8)	- 1.107 (6)
x_{333}		-5.7(5) x 10^{-3}
x_{13}	- 2.542 (1)	- 2.555 (2)
B_e	0.05831 (1)	0.05827 (1)
α_1	1.25 (1) x 10^{-4}	1.14 (1) x 10^{-4}
α_3	1.95 (1) x 10^{-4}	1.86 (2) x 10^{-4}
D_e	9.1 (15) x 10^{-9}	13.3 (21) x 10^{-9}
N° lines	1517	1829
RMS deviation	0.14	0.25
T' (level 1)	16329.59 (3)	16329.70 (6)
T' (level 2)	16704.54 (3)	16704.62 (6)

The rotational constants B_v' and D_v' for the upper state levels 1 and 2 were kept fixed at the values determined from the band by band fit (see text).

Level 1 : B' = 0.051764, D'= 8.41 x 10^{-9} Level 2 : B'= 0.051330, D' = 8.45 x 10^{-9}

data set. Higher anharmonicity terms can just be determined. The differences in the upper state vibronic energies quoted in Tables II and III arise from the implicitly different energy origins for the two fits. The band-by-band fit used the lowest observed vibrational energy level of the ground state as zero energy, whereas the polynomial model has an energy origin corresponding to $v_1'' = v_3'' = -\frac{1}{2}$. This quantity does not reflect a real zero-point energy for the molecule, because the contribution in v_2 has been neglected.

DISCUSSION

In this work, we have endeavored to understand the electronic transitions occurring in laser-induced fluorescence spectra of copper dichloride. The nature of the spectra made this task nontrivial, and even now, our picture of the ground state remains incomplete. Some of the omissions require a few words of explanation. One of the more obvious flaws in this study is that we have found no evidence at all for the bending vibration, v_2. An absence of progressions in v_2 can be explained away by claiming that both electronic states involved in the transition are linear, and that wavefunction overlaps with $\Delta v_2 \neq 0$ are very small; but even so, we would have expected to see transitions with $\Delta v_2 = 0$ corresponding to $v_2 = 1, 2$, etc. The bending vibration has been measured at 127 cm^{-1} (*14*) in the ground state, and using DCM dye, we have recorded many fluorescence series originating from a ground state level with $v_1 = 1$, which is roughly equivalent in energy to three quanta of v_2. There is thus no reason to suppose that the levels $v_2 = 1$, 2, and 3 are not thermally populated at the temperatures of our experiment ($\sim$750°C). The most probable, although not very satisfactory, explanation for this may well lie in our choice of laser wavelengths. Because we had aimed to produce a data set which was "easy" to analyze, we worked over a fairly small range of laser wavelengths within the profile of each dye. It is just possible that the difference between the upper and lower state stretching frequencies is large enough for transitions with, say, $v_2' = v_2'' \neq 0$ to have been inaccessible to our excitation lines. The same reasoning can be applied to our failure to observe the other spin–orbit component of the $^2\Pi_g$ state with a little more confidence; it is not unreasonable to postulate that the energy origins of the $^2\Pi_{u(3/2)}$–$^2\Pi_{g(3/2)}$ and $^2\Pi_{u(1/2)}$–$^2\Pi_{g(1/2)}$ transitions could be separated by more that 50 cm^{-1} by spin–orbit effects in the $CuCl_2$ molecule.

With these limitations in mind, we have analysed the vibrational features in our fluorescence spectra, and obtained reliable spectroscopic constants for rotational motion, and for the symmetric and antisymmetric stretching vibrations. We have observed two vibronic levels of the upper state, whose identities in terms of vibrational modes remain obscure, and we have assigned the discrete lines in the fluorescence spectrum to transitions from these levels to a single lower lying electronic state of $CuCl_2$. But the discrete part of the spectrum is in fact a minor component of the total fluorescence (see Fig. 2). The origin of the ever-present continuum is not at all clear. It might arise from collisional transfer of energy to neighboring electronic states, but if energy transfer were to occur whilst $CuCl_2$ is in its $^2\Pi_u$ excited state, we would normally have seen extensive rotational relaxation lines around the main fluorescence doublets, as well as the collisionally excited continuum transition. Another hypothesis is that the continuum emission comes from $CuCl_2$ dimers, which might either be excited directly by the laser ($(CuCl_2)_2$ has been reported (*14*) to absorb quite strongly around 600 nm), or else be formed by collision between a $CuCl_2$ molecule in the $^2\Pi_u$ state and a ground state molecule. Whatever its origin, this continuum can be produced by any wavelength originating from the ring laser operating with R6G or DCM. Although

this discovery seems simply to add yet another unanswered question, it was an interesting observation for another reason.

The original choice of copper dichloride as a transition metal dihalide for spectroscopic investigation was influenced by our attempts to identify the emitting species in the reaction between hot copper and chlorine in the presence of singlet oxygen ($^1\Delta_g$). The bright red emission which accompanies this reaction was first reported by Yoshida *et al.* (*9*), and has since been studied by many other groups (*10–13*). We had recorded this emission on our FT spectrometer from 650–900 nm. The emission consists of a continuum with broad vibrational peaks superposed on it. We supported the hypothesis that copper dichloride was responsible for this emission, but could not eliminate the possibility that more than one species might be involved. Now we find that the fluorescence lines from our upper level "1" to the observed component of the $^2\Pi_g$ state of $CuCl_2$ match the peaks in the emission spectrum of the red flame, and that the continuum found in the fluorescence spectra matches the continuum of the flame rather well. We intend to pursue this aspect further once we have more data pertaining to the other isotopomers of copper dichloride.

CONCLUSION

We have used a simple laser-induced fluorescence technique in combination with a traditional hot source to produce very simple, rotationally resolved electronic spectra of copper dichloride. Fourier transform spectra extending from 11 000 to 15 500 cm^{-1} revealed vibrational progressions in the totally symmetric vibration, ν_1'', and also in even quanta of the antisymmetric vibration, ν_3''. The nonappearance of vibrational levels with $v_3'' = 1, 3, 5$, etc. is governed by the symmetry of this linear molecule. Given that ν_2 and ν_3 are nontotally symmetric vibrations, only transitions with even Δv_3 and Δv_2 can exist in a progression, because the total vibrational wavefunction must be totally symmetric for the transition to be allowed. Usually, the intensity of the progression in even Δv_3 drops rapidly as v_3 increases. We cannot yet explain why we observe such a strong divergence from normal behavior in this respect. Progressions in even quanta of ν_2, which are symmetry allowed, are likely to be weak if both the upper and lower electronic states are linear, as overlap between the upper and lower state wavefunctions will be poor. We observed neither progressions nor combinations in the bending vibration.

Having identified the vibrational structure present in our fluorescence spectra, we derived molecular constants for the ground state, $^2\Pi_g$, of the $^{63}Cu\,^{35}Cl_2$ molecule, both on a band-by-band basis and in the form of a simple polynomial expression. The differences between the energies associated with the three normal vibrational modes are such that we have been able to ignore Fermi resonances at this stage, and can represent the vibrational energies of levels up to about 2500 cm^{-1} ($v_1'' < 8$) involving the symmetric and antisymmetric stretching vibrations by their fundamental frequencies and first-order anharmonicity terms. Only the anharmonicity constant x_{13} couples these two vibrations in this model, which nonetheless recalculates all fluorescence lines occurring to these vibrational levels to within 0.15 cm^{-1}.

ACKNOWLEDGMENTS

We thank Mr. B. Erba, who made a series of $CuCl_2$ cells for us. We are also grateful to Dr. J. M. Brown and his collaborators for helpful discussions based on their experience with nickel dichloride, and to Dr. C. Linton for his critical reading of the manuscript. The Fourier transform interferometer was financed jointly by the CNRS, Université Lyon I, and the Région Rhone Alpes. This work benefitted from financial support

from the Air Force Office of Scientific Research (Grant AFOSR-91-0235) and from the Direction des Recherches, Etudes et Techniques (Grant 901609/A000/DRET/DS/SR).

RECEIVED: July 31, 1992

REFERENCES

1. A. J. BOUVIER, R. BACIS, J. BONNET, S. CHURASSY, P. CROZET, B. ERBA, J. B. KOFFEND, J. LAMARRE, M. LAMRINI, D. PIGACHE, AND A. J. ROSS, *Chem. Phys. Lett.* **184,** 133–140 (1991).
2. C. W. BAUSCHLICHER AND B. O. ROOS, *J. Chem. Phys.* **91,** 4785–4792 (1989).
3. C. W. DECOCK AND D. M. GRUEN, *J. Chem. Phys.* **44,** 4387–4398 (1966).
4. L. R. ZINK, J. M. BROWN, T. R. GILSON, AND I. R. BEATTIE, *Chem. Phys. Lett.* **146,** 501–506 (1988).
5. L. R. ZINK, F. J. GRIEMAN, J. M. BROWN, T. R. GILSON, AND I. R. BEATTIE, *J. Mol. Spectrosc.* **146,** 225–237 (1991).
6. S. ASHWORTH, F. J. GRIEMAN, AND J. M. BROWN, *Chem. Phys. Lett.* **175,** 660–666 (1990).
7. A. BÜCHLER, J. STAUFFER, AND W. KLEMPERER, *J. Chem. Phys.* **40,** 3471–3474 (1964).
8. A. J. BOUVIER, R. BACIS, J. BONNET, S. CHURASSY, P. CROZET, B. ERBA, J. B. KOFFEND, J. LAMARRE, M. LAMRINI, D. PIGACHE, AND A. J. ROSS, *J. Phys. IV* **C7,** 663–666 (1991).
9. S. YOSHIDA, M. TANIWAKI, T. SAWANO, K. SHIMIZU, AND T. FUJIOKA, *J. Appl. Phys. Jpn.* **28,** L831–L833 (1989).
10. S. YOSHIDA, K. SHIMIZU, T. SAWANO, T. TOKUDA, AND T. FUJIOKA, *Appl. Phys. Lett.* **54,** 2400–2402 (1989).
11. T. TOKUDA, N. FUJII, S. YOSHIDA, K. SHIMIZU, AND I. TANAKA, *Chem. Phys. Lett.* **174,** 385–388 (1990).
12. R. BACIS, J. BONNET, A. J. BOUVIER, P. CROZET, S. CHURASSY, E. GEORGES, B. ERBA, J. LAMARRE, Y. LOUVET, M. NOTA, D. PIGACHE, A. J. ROSS, AND M. SETRA, *Europhys. Lett.* **12,** 569–574 (1990).
13. H. P. YANG, Y. QIN, T. J. CUI, Q. N. YUAN, X. B. XIE, Q. ZHUANG, AND C. H. ZHANG, *Chem. Phys. Lett.* **191,** 130–135 (1992).
14. F. DIENSTBACK, F. P. EMMENEGGER, AND C. W. SCLAPHER, *Helv. Chem. Acta* **60,** 2460–2470 (1977).